RESEARCH ARTICLE

The TP53 Apoptotic Network Is a Primary Mediator of Resistance to BCL2 Inhibition in AML Cells

Tamilla Nechiporuk[1,2], Stephen E. Kurtz[1,2], Olga Nikolova[2,3], Tingting Liu[1,2], Courtney L. Jones[4], Angelo D'Alessandro[5], Rachel Culp-Hill[5], Amanda d'Almeida[1,2], Sunil K. Joshi[1,2], Mara Rosenberg[1,2], Cristina E. Tognon[1,2,6], Alexey V. Danilov[1,2], Brian J. Druker[1,2,6], Bill H. Chang[2,7], Shannon K. McWeeney[2,8], and Jeffrey W. Tyner[1,2,9]

ABSTRACT

To study mechanisms underlying resistance to the BCL2 inhibitor venetoclax in acute myeloid leukemia (AML), we used a genome-wide CRISPR/Cas9 screen to identify gene knockouts resulting in drug resistance. We validated *TP53*, *BAX*, and *PMAIP1* as genes whose inactivation results in venetoclax resistance in AML cell lines. Resistance to venetoclax resulted from an inability to execute apoptosis driven by BAX loss, decreased expression of BCL2, and/or reliance on alternative BCL2 family members such as BCL2L1. The resistance was accompanied by changes in mitochondrial homeostasis and cellular metabolism. Evaluation of *TP53* knockout cells for sensitivities to a panel of small-molecule inhibitors revealed a gain of sensitivity to TRK inhibitors. We relate these observations to patient drug responses and gene expression in the Beat AML dataset. Our results implicate *TP53*, the apoptotic network, and mitochondrial functionality as drivers of venetoclax response in AML and suggest strategies to overcome resistance.

SIGNIFICANCE: AML is challenging to treat due to its heterogeneity, and single-agent therapies have universally failed, prompting a need for innovative drug combinations. We used a genetic approach to identify genes whose inactivation contributes to drug resistance as a means of forming preferred drug combinations to improve AML treatment.

See related commentary by Savona and Rathmell, p. 831.

[1]Division of Hematology and Medical Oncology, Oregon Health and Science University, Portland, Oregon. [2]Knight Cancer Institute, Oregon Health and Science University, Portland, Oregon. [3]Department of Biomedical Engineering, Oregon Health and Science University, Portland, Oregon. [4]Division of Hematology, University of Colorado Denver, Aurora, Colorado. [5]Department of Biochemistry and Molecular Genetics, University of Colorado Denver, Aurora, Colorado. [6]Howard Hughes Medical Institute, Oregon Health and Science University, Portland, Oregon. [7]Department of Pediatrics, Oregon Health and Science University, Portland, Oregon. [8]Division of Bioinformatics and Computational Biology, Department of Medical Informatics and Clinical Epidemiology, Oregon Health and Science University, Portland, Oregon. [9]Department of Cell, Developmental and Cancer Biology, Knight Cancer Institute, Oregon Health and Science University, Portland, Oregon.

Note: Supplementary data for this article are available at Cancer Discovery Online (http://cancerdiscovery.aacrjournals.org/).

Corresponding Author: Jeffrey W. Tyner, Oregon Health and Science University, 3181 SW Sam Jackson Park Road, Mailcode KR-HEM, Portland, Oregon 97239. Phone: 503-346-0603; Fax: 503-494-3688; E-mail: tynerj@ohsu.edu.

Cancer Discov 2019;9:910–25

doi: 10.1158/2159-8290.CD-19-0125

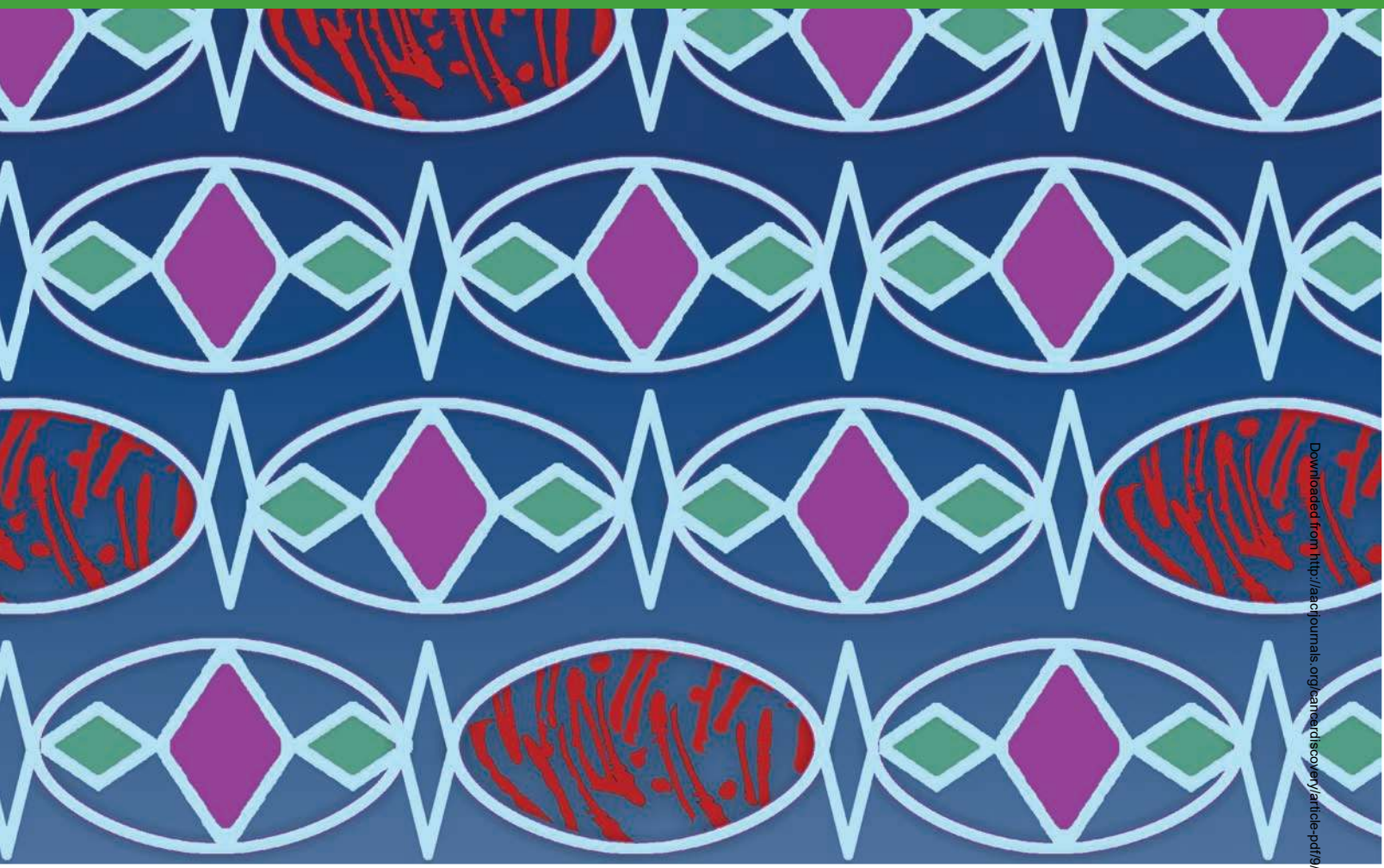

INTRODUCTION

Resisting cell death is a hallmark of cancer as well as an essential feature of acquired drug resistance (1–3). To maintain their growth and survival, cancer cells often modulate cell death mechanisms by overexpression of antiapoptotic BCL2 family members, including BCL2, BCL2L1, and MCL1. This overexpression aims to neutralize BH3 domains of the apoptotic activators BID, BIM, and PUMA, thus preventing liberation of the proapoptotic proteins BAX and BAK from inhibitory interactions with antiapoptotic BCL2 family proteins (4–6). Elevated levels of MCL1 protein are commonly observed in cancer and are associated with poor survival in myeloid hematologic malignancies (7–10). Aberrant prosurvival regulation can also be achieved by inactivation of p53 function, which controls many aspects of apoptosis (11, 12). These processes alter the balance of proapoptotic and antiapoptotic proteins, permitting cancer cells, otherwise primed for apoptosis, to survive and resist therapies.

The elucidation of BH3 protein family interactions involved in promoting or inhibiting apoptosis has enabled the development of small-molecule inhibitors targeting specific antiapoptotic family members leading to release of the proapoptotic proteins BAX and BAK, their oligomerization and mitochondrial outer membrane permeabilization, and ultimately execution of the irreversible apoptotic cascade (13–17). The latest generation of BH3 mimetics, venetoclax, selectively targets BCL2, thus overcoming the deficiencies and side effects of its predecessors, navitoclax and ABT-737, which targeted BCL2 and BCL2L1. Selective MCL1 inhibitors have also been developed and are in clinical development (18–20). Venetoclax has FDA approval for use in patients with chronic lymphocytic leukemia (CLL), and its efficacy has been evaluated for other hematologic malignancies; it has been recently approved in combination with a hypomethylating agent for acute myeloid leukemia (AML; refs. 21–25). Intrinsic or acquired resistance is a central concern with single-agent targeted therapies, with many instances now documenting favorable initial responses that give way to disease relapse resulting from loss of drug sensitivities (26).

For venetoclax, both acquired and intrinsic resistance is anticipated from initial clinical studies using venetoclax monotherapy on patients with relapsed/refractory AML, which have shown modest efficacy due to either intrinsic or acquired drug resistance (24). The efficacy of venetoclax in patients with AML is dependent on BCL2 expression levels, and resistance to venetoclax may result from overexpression of the antiapoptotic proteins MCL1 or BCL2L1 (21, 24). Similar mechanisms have been observed in lymphoma cell lines, as several studies have shown resistance to venetoclax developing primarily through alterations in levels of other antiapoptotic

proteins (27, 28). AML cell lines rendered resistant to venetoclax through prolonged exposure develop a dependency on MCL1 or BCL2L1 (19, 29). In AML cells, the dependency on MCL1 for survival can be overcome by MAPK/GSK3 signaling via activation of p53, which when coupled with BCL2 inhibition enhances the antileukemic efficacy of venetoclax (30).

Drug combinations offer a strategy to overcome limitations in the durability and overall effectiveness of targeted agents resulting from intrinsic mechanisms of resistance. Understanding these mechanisms is essential for identifying drug targets that will form the basis for new combinatorial therapeutic strategies to circumvent drug resistance. To identify essential target genes and pathways contributing to venetoclax resistance in AML, we used a genome-wide CRISPR/Cas9 screen on an AML patient–derived cell line, MOLM-13. Our findings identify *TP53*, *BAX*, and *PMAIP1* as key genes whose inactivation establishes venetoclax resistance, centering on regulation of the mitochondrial apoptotic network as a mechanism of controlling drug sensitivity. Cell lines with *TP53* or *BAX* knockouts (KO) show perturbations in metabolic profile, energy production, and mitochondrial homeostasis. In addition, *TP53* KO cells acquired sensitivity to TRK inhibitors, suggesting a new dependency on this survival pathway, indicating changes in transcriptional activity in the venetoclax-resistant setting may offer drug combinations to overcome resistance.

RESULTS

Genome-Wide Screen Reveals p53 Apoptosis Network Controlling Venetoclax Resistance

To understand possible mechanisms of venetoclax resistance in the setting of AML, we screened an AML cell line, MOLM-13, which harbors the most common genetic lesion observed in AML (FLT3-ITD), for loss-of-function genes conferring venetoclax resistance. We initially generated Cas9-expressing MOLM-13 cells as described (ref. 31; Fig. 1A) and confirmed Cas9 functionality (Fig. 1B). Systematic genetic perturbations on a genome-wide scale were introduced by infecting Cas9-expressing cells with lentiviruses carrying a CRISPR library consisting of an average of 5 single-guide RNAs (sgRNA) per gene for 18,010 genes, hereafter referred to as Y. Kosuke (31). After transduction, we further selected cells with puromycin for 5 days to ensure stable guide integration, and then subjected cells to treatment with either 1 μmol/L venetoclax or vehicle alone (DMSO) for 14 days while collecting DNA at various time points (Fig. 1C). By day 7 of drug treatment, venetoclax reduced cell viability by approximately 50% relative to 75% reduction without drug exposure. PCR-amplified libraries of barcodes representing unique sgRNA sequences obtained from DNA extracted from either control (DMSO) or drug-treated cells were subjected to deep sequencing and analyzed using a MAGeCK pipeline analysis (ref. 32; Fig. 1D; Supplementary Tables S1 and S2). Plotting the average log fold change for sgRNA counts per gene versus cumulative *P* values generated by robust rank aggregation analyses revealed a high enrichment of p53 and BAX in venetoclax-resistant populations as well as a significant enrichment for several other genes involved in the apoptosis pathway or mitochondrial homeostasis, such as *PMAIP1* (*NOXA*), *TFDP1*, and *BAK1* (*BAK*; Fig. 1E). These findings are concordant with results of a similar screen, described in a companion paper by Chen and colleagues in this issue. To confirm our results, we performed a parallel screen in MOLM-13 cells using a distinct genome-wide library, Brunello (33), which also identified *TP53*, *BAX*, and *PMAIP1* among the top-enriched sgRNAs (Fig. 1F; Supplementary Tables S1 and S2). The distribution of concordance, defined as a statistically significant increase or decrease ($P < 0.05$) in the same direction among all sgRNAs for a given gene, showed higher average percent concordance in the Y. Kosuke library screen compared with the Brunello library screen (0.77 ± 0.07, $n = 916$ vs. 0.62 ± 0.004, $n = 2310$, unpaired two-tailed *t* test, $P < 0.0001$); therefore, we focused on the Y. Kosuke screen results for pathway analyses. Ranking genes with statistically significant enriched sgRNAs ($P < 0.05$) based on concordance as described above and a ≥3 log fold change compared with controls identified 234 genes (Supplementary Table S3). Functional enrichment analyses of these 234 candidates indicated an enrichment in genes involved in mitochondrial processes, such as apoptosis transcriptional regulation (*TP53* and *TFDP1*; refs. 13 and 34) and apoptosis sensitization [*PMAIP1* (*NOXA*); ref. 35], genes required for mitochondrial membrane pore formation (*BAX*, *BAK, SLC25A6*, and *TMEM14A*; refs. 13, 34), and additional genes involved in apoptosis (proapoptotic *BNIP3L*; ref. 36; Supplementary Table S4). The top-enriched sgRNAs showed a high degree of concordance in fold change relative to controls (Fig. 1G; Supplementary Tables S1 and S2) and had a baseline of more than 100 normalized counts in control samples, precluding artificial inflation of fold changes in resistant cells (Fig. 1H).

Prioritization of Genome-Wide Screen Candidates

Our study used two independent sgRNA guide libraries, which provided a high degree of confidence with respect to the top hits identified. Analysis of genome-wide CRISPR screen knockouts is challenged by off-targeting, sgRNA guide efficiency, and other factors that can lead to library-specific artifacts and striking differences between libraries (31, 33). To prioritize candidates for validation, we developed a tier structure that incorporates three key factors: evidence (determined by the number of sgRNA guide hits per gene), concordance (indicated by the agreement across the set of guides for a given gene), and discovery (based on expanding effect size threshold) to rank sgRNA hits and enable a progression to pathway analysis for lower-scoring hits (Supplementary Methods). Using this prioritization scheme, the tier 1 hits ($n = 149$) revealed significant biological identity with the *TP53* Regulation of cytochrome C release pathway (Reactome; corrected $P < 0.001$), which is concordant with our initial analysis.

Inactivation of Genes as Single Knockouts Confirms Resistance to Venetoclax and Validates the Screen

To validate the screen hits, we designed several individual sgRNAs to knock out *TP53, BAX, PMAIP1, TFDP1*, and several other top candidate genes along with nontargeting controls. Analyses of drug sensitivity at 14 days after transduction of MOLM-13 cells with individual sgRNAs revealed a loss of

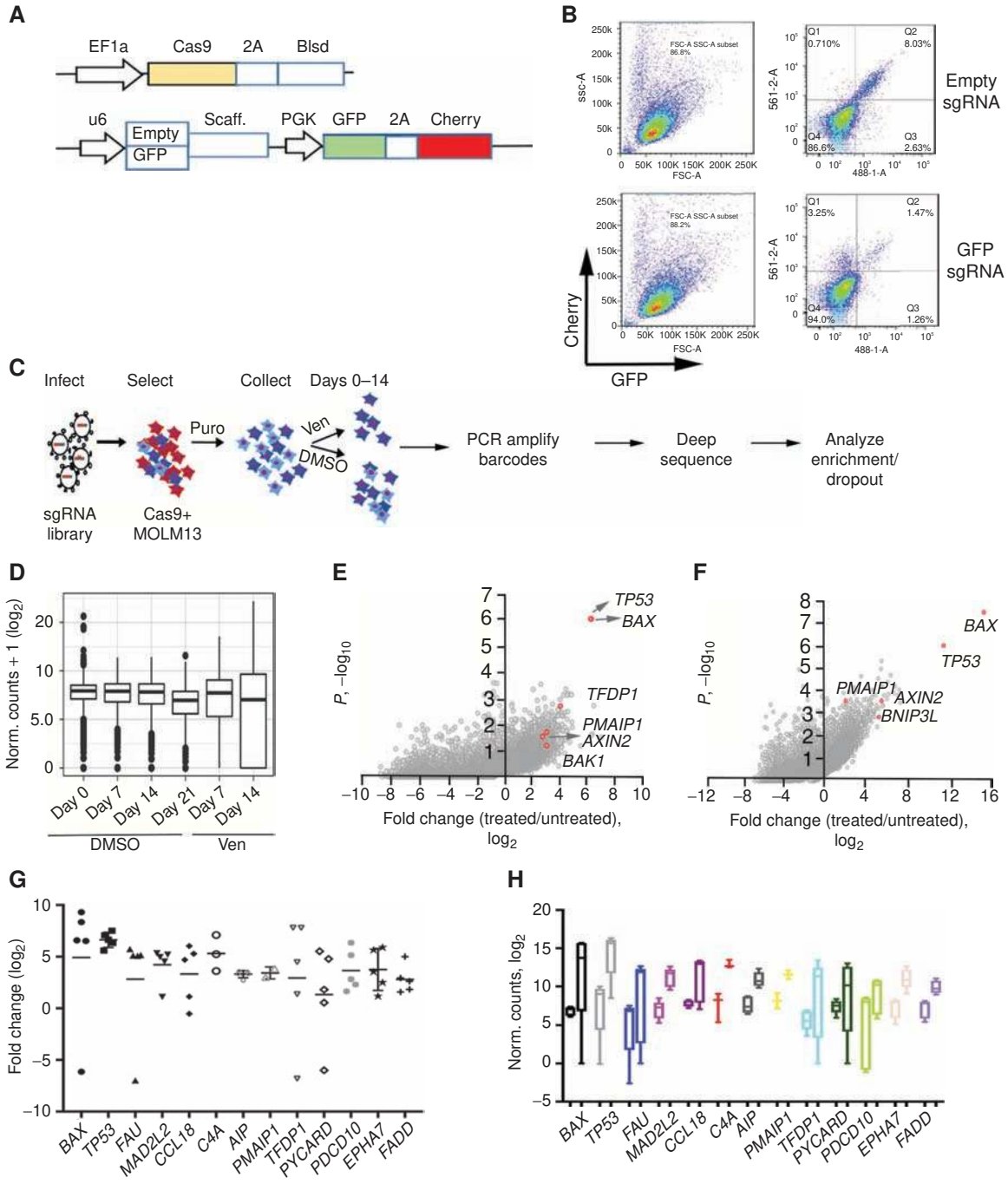

Figure 1. Genome-wide CRISPR/Cas9 screen in AML cells identified *TP53*, *BAX*, and other apoptosis network genes conferring sensitivity to venetoclax. **A,** Schematic representation of lentiviral vectors described elsewhere in detail (31) and used for the delivery and functional assay of Cas9. Top, Cas9-expressing vector; Blsd, blasticidin selection gene; EF1a, intron-containing human elongation factor 1a promoter; Cas9, codon-optimized Streptococcus pyogenes double-NLS-tagged Cas9; 2A, *Thosea asigna* virus 2A peptides. Bottom, vector carrying dual fluorescent proteins; GFP and mCherry expressed from the PGK promoter; U6 denotes human U6 promoter driving GFP sgRNAs or empty cassette; Scaff denotes sgRNA scaffold. **B,** Functional assay for Cas9 activity in MOLM-13 cells transduced with virus carrying an empty sgRNA cassette (top) or sgRNA targeting GFP (bottom), assessed by flow cytometry 5 days after transduction. Note the significant decrease in GFP signal in the presence of sgRNA targeting GFP. **C,** Schematic representation of genome-wide screen for drug resistance. The sgRNA library (31) was transduced into Cas9-expressing MOLM-13 cells, selected with puromycin for the integration of sgRNA-carrying virus for 5 days and DNA collected from cells exposed to venetoclax (1 μmol/L) or vehicle (DMSO) for various time points (days 0, 7, 14, and 21). sgRNA barcodes were PCR-amplified and subjected to deep sequencing to analyze for enrichment and/or dropout. **D,** Normalized counts of sgRNAs from collected DNA samples, median, upper, and lower quartiles are shown for representative replicate samples. **E, F,** Enrichment effect in Y. Kosuke (**E**) and Brunello (**F**) library screens for loss of sensitivity to venetoclax. Fold change and corresponding *P* values are plotted; genes representing significant hits in both libraries are highlighted in red. **G,** Enrichment extent plotted as fold change over control following venetoclax exposure (day 14) for the set of individual top hit sgRNAs per gene is shown (Y. Kosuke library). **H,** Box and whisker plots spanning min/max values of normalized counts for control (left boxes in each pair) and venetoclax treatment (right boxes in each pair) combined for all sgRNAs per gene. Top hits are shown.

venetoclax sensitivity (Fig. 2A). The top candidates, including *TP53* and *BAX*, were also validated by single-guide inactivation in an additional cell line, MV4-11 (Fig. 2B and C), with many IC_{50} values significantly exceeding initial drug concentrations used for the sgRNA screen. Analyses of protein levels for the top candidates, *BAX*, *TP53*, and *PMAIP1*, demonstrated significant loss of protein upon sgRNA inactivation (Fig. 2D; Supplementary Fig. S1A and S1B). Although *BAX* is reported to be a p53 transcriptional target (reviewed in ref. 37), its levels remained unchanged when *TP53* was inactivated, indicating that other transcriptional factors may regulate BAX levels in these cells (38). Levels of other p53 target gene products such as PMAIP1, PUMA, and BAK1 were decreased in *TP53* KO cells (Supplementary Fig. S1A and S1C). At the same time, levels of antiapoptotic proteins BCL2 and MCL1 were reduced in all four tested *TP53* knockout lines, inversely correlating with increased BCLXL expression (Fig. 2D; Supplementary Fig. S1C). Analysis of protein levels revealed increases in the ratios of BCLXL to BCL2 in *TP53* KO cells (Supplementary Fig. S1D). Venetoclax directly binds BCL2; therefore, a decrease in BCL2 expression in *TP53* KO cells may contribute to the loss of sensitivity. The inverse correlation of low BCL2/high BCLXL expression with null *TP53* status is similarly observed in pediatric acute lymphoblastic leukemia (39). In a large AML patient cohort (Beat AML; ref. 40), BCL2 expression positively correlated with *TP53* expression, whereas both BCLXL and MCL1 had inverse correlations (Fig. 2E). Increased levels of BCLXL in *TP53* KO cells correlate with sensitivity to a BCL2/BCLXL inhibitor (AZD-4320; Fig. 2F). Because both MOLM-13 and MV4-11 cell lines carry an FLT-ITD mutation, we introduced loss-of-function mutations in *TP53*, *BAX*, and *PMAIP1* into OCI-AML2, an FLT3 wild-type (WT) cell line, and observed similarly diminished sensitivities to venetoclax (Supplementary Fig. S1E and S1F).

AML Patient Samples with Mutant *TP53* Status or Low Expression Levels of *TP53* and *BAX* Have Diminished Sensitivity to Venetoclax *Ex Vivo*

To assess whether the top candidates from the screen have a direct relevance to gene perturbation in patients with AML, we analyzed the correlation of venetoclax drug sensitivity with gene-expression levels and mutational status using the Beat AML patient sample dataset (40). Our analyses indicated that 16 patient samples harboring deleterious *TP53* mutations showed a trend toward reduced venetoclax sensitivity (measured as increases in AUC in a nonlinear modeling of drug response curves) compared with 282 AML patient samples with WT *TP53* (Mann–Whitney *t* test, $P < 0.04$; Fig. 3A). Furthermore, separation of *TP53* expression levels into high and low quartiles across the total *TP53* WT cohort showed high quartile samples were more sensitive to venetoclax than low quartile samples (Fig. 3B). Regardless of *TP53* mutational status, both *TP53* and *BAX* expression levels were inversely correlated with venetoclax sensitivity (high AUC), underscoring the relevance of our CRISPR-derived loss-of-function candidates to patient-level responses *ex vivo* (Fig. 3C). As expected, BCL2 levels showed an inverse correlation with venetoclax sensitivity, whereas BCLXL expression directly correlated with venetoclax sensitivity (Fig. 3C).

Inactivation of *TP53* and *BAX* Diminishes the Apoptotic Response to Venetoclax

To characterize venetoclax sensitivity in MOLM-13 cells with KOs for *TP53*, *BAX*, or *PMAIP1*, we evaluated an early marker of apoptosis by measuring the percentage of Annexin V–positive cells in response to venetoclax treatment (100 nmol/L) (41). Cells with KOs for *TP53*, *BAX*, or *PMAIP1* showed a significant decrease in the number of cells undergoing apoptosis (Fig. 4A and B). This was accompanied by sustained phosphorylation of MAPK1/3 (ERK1/2) during venetoclax treatment and increase in total levels of AKT and MAPK1/3 in cells with inactivation of *TP53* and *BAX* (Fig. 4C).

Resistance to Venetoclax Coincides with Protection from Mitochondrial Stress and Increases in Oxidative Phosphorylation

The top hits from our CRISPR screen pointed toward perturbations in mitochondrial regulators and effectors of the apoptotic program. p53, BAX, PMAIP1, TFDP1, and BAK function in a proapoptotic manner: p53 acts a sensor of cellular stress and transcriptional regulator of several proapoptotic genes; TFDP1 activates and translocates PMAIP1 into the mitochondria; PMAIP1 promotes activation of the apoptotic program; and BAX/BAK function as its effectors. In this manner, we observed that inactivation of *TP53* led to alterations in the expression of antiapoptotic BCL2 family members and many *TP53* transcriptional targets that affect mitochondrial homeostasis and cellular metabolism (Fig. 2D; Supplementary Fig. S1). *TP53* inactivation also altered response to a variety of stress stimuli and rendered cells resistant to many other pharmacologic agents. These changes prompted us to investigate the impact of overall response to mitochondrial stress in cells briefly exposed to venetoclax (Fig. 5A–D). Cells with inactivation of p53 and *BAX* were less likely to undergo mitophagy in response to the mitochondrial uncoupler carboyl cyanide m-chlorophenyl hydrazine (CCCP), regardless of venetoclax treatment, with more pronounced protection observed in *TP53* mutants, suggesting overall changes in mitochondrial homeostasis (Fig. 5A and B). Additionally, *TP53*- and *BAX*-mutant cells were less likely to lose mitochondrial membrane potential in response to CCCP alone, with venetoclax potentiating the CCCP uncoupling action (Fig. 5C and D).

Venetoclax inhibits BCL2 by mimicking the BH3 binding of apoptotic sensitizers/activators. Both venetoclax and chemical inhibition of BCL2 influence energy production by decreasing oxidative phosphorylation in the mitochondria of leukemia stem cells (42) and can affect various metabolic activities in the cells, including amino acid catabolism (43). In addition, we observed reduced levels of PUMA in *TP53* KO cells (Supplementary Fig. S1C), recently identified as a p53-induced metabolic switch (44). Because p53 regulates many genes whose products determine the balance of reactive oxygen species (ROS) production in response to cellular stress (45–47), we evaluated whether oxidative phosphorylation was perturbed in cells inactivated for *TP53* by measuring rates of oxygen consumption and electron transport across the mitochondrial membrane. Both outputs were enhanced in mutant cells (Fig. 5E and F), accompanied by a moderate

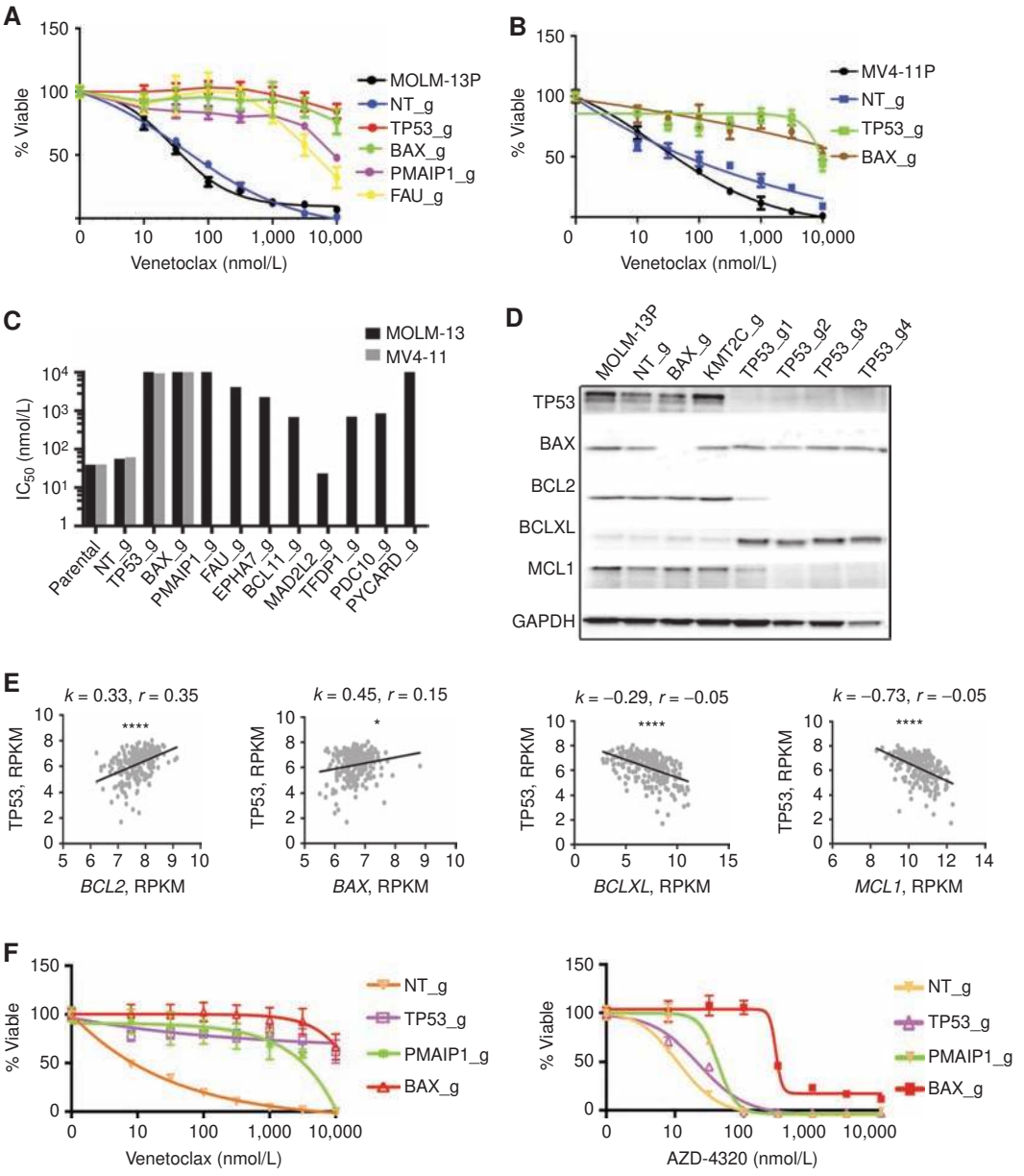

Figure 2. **A,** Confirmation of genes conferring venetoclax resistance in MOLM-13 and MV4-11 cells and correlations with changes in apoptotic gene transcription in patients with AML. MOLM-13 (**A**) or MV4-11 (**B**) cells were transduced with lentiviruses carrying single sgRNA/Cas9 constructs targeting *TP53, BAX, PMAIP1, FAU*, or control (nontargeting; NT_g). Ten days after transduction, venetoclax sensitivity was measured in triplicate by colorimetric MTS assay using a 7-point concentration range (10 nmol/L to 10 μmol/L). Percentages of viable cells, after normalization to untreated controls, were fit using nonlinear regression analyses; mean and standard errors are shown. MOLM-13P, parental MOLM-13 cells; MV4-11P, parental MV4-11 cells. **C**, Histogram (log scale) summarizing IC_{50} estimates from triplicate measurements for venetoclax sensitivity in parental MOLM-13 (black shaded), parental MV4-11 cells (gray shaded), or cells transduced with indicated sgRNA/Cas9 viruses. **D,** Western blot analyses of proteins extracted from MOLM-13 cells, transduced with indicated sgRNA/Cas9 viruses, and identified with antisera to BAX, BCL2, BCLXL, MCL1, and GAPDH. Note that for *TP53*, four sgRNAs producing distinct knockout alleles were used to confirm changes in expression levels of BCL2, BCLXL, and MCL1. sgRNA targeting *KMT2C* was used as an additional unrelated sgRNA control. **E,** Correlation of expression of *TP53* and selected genes in an AML patient sample cohort ($n = 246$; ref. 40). k, slopes generated by linear regression; *r*, Spearman coefficient; *, $P < 0.05$; ****, $P < 0.0001$. **F**. Sensitivity profiles of venetoclax (left) and AZD-4320 (right) on MOLM-13 cells transduced with lentiviruses carrying single sgRNA/Cas9 constructs targeting *TP53, BAX, PMAIP1*, and NT (nontargeting) control, measured as in **A** using a 7-point concentration range (8 nmol/L to 10 μmol/L).

increase in cellular ROS (Fig. 5G), as oxidative phosphorylation is a major cellular source of ROS production (48). Interestingly, both *TP53* and *BAX* KO cells were still susceptible to cell death by elesclomol, a drug that induces cellular death through an increase in cellular oxidation (49), suggesting that apoptosis can still be triggered in venetoclax-resistant cells through disruption of mitochondrial homeostasis (Fig. 5H). These results suggest an inhibition of a general mitochondrial stress response coupled with increased cellular respiration.

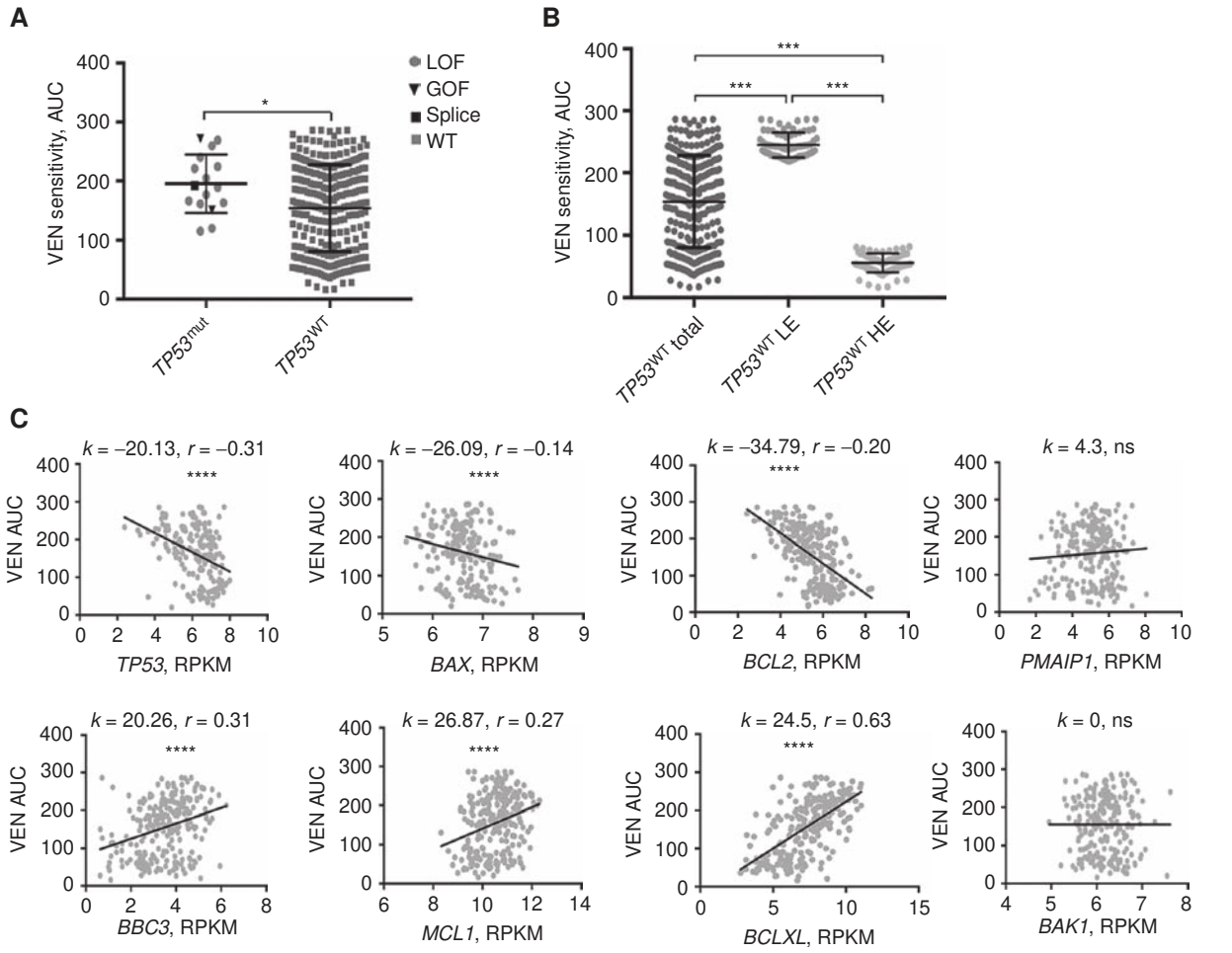

Figure 3. Venetoclax (VEN) sensitivity in patients with AML inversely correlates with *TP53* mutations and low expression of *TP53* and *BAX*. **A,** Comparison of VEN sensitivity between *TP53*-mutant ($TP53^{mut}$; $n = 16$) and *TP53* WT ($TP53^{WT}$; $n = 282$) patient samples (Mann–Whitney, two-tailed). Within *TP53*-mutant groups, circles, triangles and square symbols denote loss of function (LOF), gain of function (GOF), and splice variants correspondingly. **B,** Comparison of VEN sensitivity between the lowest expressing (LE; $n = 71$) and highest expressing (HE; $n = 71$) quartiles for *TP53* in WT patient samples. Median expression levels for both LE and HE groups differ significantly from the median expression levels in all samples (ANOVA with Tukey post-test). **C,** Correlation between gene-expression levels from AML patient samples for the indicated genes and venetoclax sensitivities represented by AUC ($n = 246$; ref. 40). k, slope values generated by linear regression; *r*, Spearman coefficient. *, $P < 0.05$; ***, $P < 0.001$ ****; $P < 0.0001$; ns, not significant.

Perturbations in the Metabolic Profile of Venetoclax-Resistant Cells

Unlike the Warburg effect where rapidly proliferating cancer cells in glucose-rich conditions switch to less efficient aerobic glycolysis using the pentose phosphate shunt (48), increased oxygen consumption in *TP53* KO cells suggests increased energy production via anaerobic glycolysis in venetoclax-resistant cells. Accordingly, we performed a global metabolomics analysis of MOLM-13 cells with inactivation of *TP53*, *BAX*, and nontargeting controls. Unexpectedly, we observed a significant decrease in major glycolysis intermediates, such as D-glucose and D-glucose-6-phosphate; however, levels of pyruvate, the final metabolite entering into the tricarboxylic acid (TCA) cycle, remained unperturbed (Fig. 6A and B; Supplementary Fig. S2; Supplementary Table S5). We also observed a decrease in levels of 6-phospho-D-gluconate, but not in subsequent intermediates in the pentose phosphate pathway (Supplementary Fig. S2; Supplementary Table S5). Additionally, a decrease in amino acid levels and urea cycle intermediates highlighted the most significantly affected pathways (Fig. 6A–D) in both *BAX*- and *TP53*-mutant cells in comparison with control cells. These reductions were accompanied by increases in nucleotide synthesis, suggesting the utilization of more glucose and amino acids for the purpose of nucleotide synthesis and cellular proliferation (Fig. 6C and D; Supplementary Table S5). We also performed parallel metabolomic studies on *TP53*-mutant and WT patient samples (Supplementary Fig. S3A–S3C; Supplementary Table S5) and found concordance for decreases in glucose and pyruvate levels, amino acids, and urea cycle intermediates (Supplementary Fig. S3A, 3B, 3D, and 3E), offering validation of the altered metabolic states observed in the cell line models (Supplementary Fig. S3). These results, together with the diminished sensitivity to venetoclax and perturbations in mitochondrial responses, illustrate the significance of our screen hits as depicted in Fig. 6E. From the transcriptional

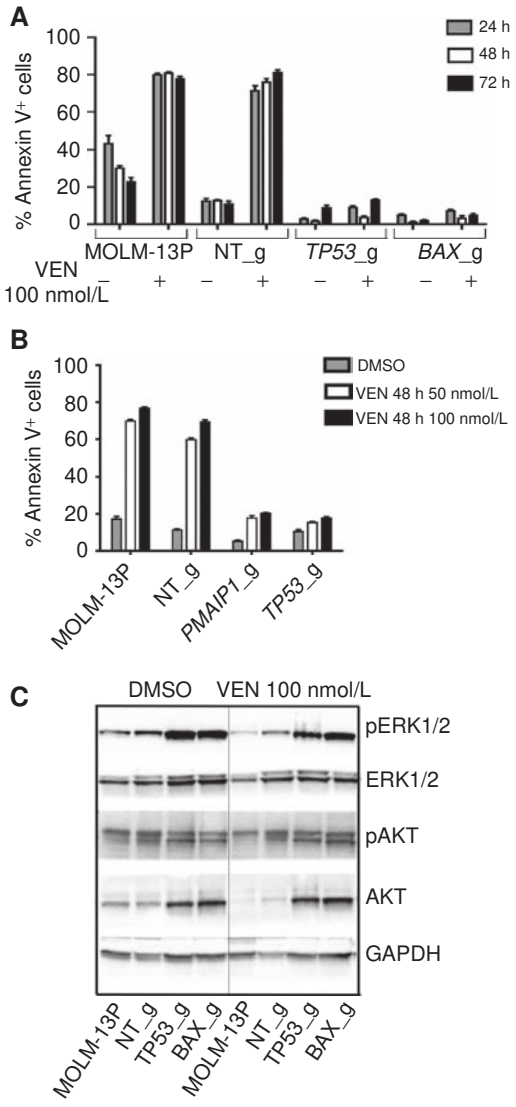

Figure 4. Cells with loss-of-function alleles for *TP53, PMAIP1*, or *BAX* have diminished apoptosis in response to venetoclax treatment. **A** and **B,** Sensitivities to venetoclax in MOLM-13 parental cells (MOLM-13P) and MOLM-13 cells with sgRNA-inactivated alleles, as indicated, were assessed by flow cytometry after staining with the early apoptosis marker, Annexin V, following 24, 48, and 72 hours of exposure to venetoclax. Histogram represents mean and standard deviation for three replicates of percentage of Annexin V$^+$ cells in the total cell population. **C,** Western blot analysis of proteins extracted from MOLM-13 parental and MOLM-13 cells transduced with indicated sgRNA/Cas9 viruses and treated overnight with 100 nmol/L venetoclax or vehicle (DMSO), and identified with antisera to phosphorylated ERK1/2 (pERK1/2; Thr202/Tyr204), ERK1/2, phosphorylated AKT (pAKT; Thr308), AKT, and GAPDH.

machinery initiated by p53 in response to cellular stress to various sensitizers such as PMAIP1 and TFDP1 to downstream mitochondrial pore effectors such as BAX, BAK, SLC25A6, and TMEM14A, our hits demonstrate the central involvement of mitochondria in conferring venetoclax sensitivity. Resistance may result from alterations in any of these components, for example, *TP53* mutation affecting BCL2 and BCL2L1 expression (Fig. 6F) or BAX loss of function affecting mitochondrial outer membrane pore formation (Fig. 6G).

Alteration of Drug Sensitivities in *TP53* and *BAX* KO Cells

To evaluate whether the mitochondrial and metabolic changes led to alterations in additional signaling pathways, we evaluated drug sensitivities in MOLM-13 and MV4-11 cells with *TP53* and *BAX* KOs relative to parental and nontargeting control cells using a panel of small-molecule inhibitors that target a variety of distinct signaling pathways activated in cancers. We observed many commonly altered drug responses among venetoclax-resistant cell lines, including a core of drug responses that were common to both modified MOLM-13 and MV4-11 cells (Fig. 7A; Supplementary Table S6). In addition to loss of venetoclax sensitivities, tyrosine kinase inhibitor sensitivities to the AKT/PI3K pathway (GDC-0941, PI-103), as well as YM-155, an inhibitor of survivin, were decreased (Fig. 7A; Supplementary Table S6). Although the *BAX* KO showed a similar sensitivity to the MCL1 inhibitor AZD5991 relative to control cells, AZD5991 sensitivity was diminished in *TP53* KO MOLM-13 cells, indicating that these cells may not depend on MCL1 for survival. The MCL1 dependency further decreased in prolonged *TP53* KO cultures, possibly due to compensatory mechanisms of survival. Except for venetoclax, few, if any, inhibitors showed concordant changes between *BAX*-inactivated MV4-11 and MOLM-13 cells (Supplementary Table S6). Additional changes for cells with *TP53* inactivation included the loss of sensitivity to all six tested FLT3 inhibitors (crenolanib, sorafenib, sunitinib, quizartinib, midostaurin, and gilteritinib; Fig. 7B; Supplementary Fig. S4A). Cells with *TP53* KO showed sustained gain of sensitivity to several NTRK/ALK/ROS1 inhibitors, namely, entrectinib (50), crizotinib (51, 52), GW-2580 (53), and AZD1480 (ref. 54; Fig. 7A, C and D; Supplementary Fig. S4B; Supplementary Table S6). Neurotropin receptors (NTRK1/2/3, also known as TRKA/B/C) are well documented to play a role in neuronal development. NTRK receptors bind neurotrophin ligands and are single transmembrane catalytic receptors with intracellular tyrosine kinase activity. NTRK receptors have recently gained attention for their oncogenic role in a variety of cancer types, occurring as a component of fusion genes (55–58). NTRK receptor activation is coupled to RAS/MAPK, PI3K, or PLCγ signaling pathways to promote survival and proliferation (58, 59). Although some TRK inhibitors have additional targets beyond NTRKs, such as ALK and ROS1, additional testing with a more selective TRK inhibitor, larotrectinib, also revealed a profound gain of sensitivity, indicating new dependences on the NTRK pathway for cell survival (Fig. 7C and D). To test whether NTRK transcripts were upregulated in *TP53* knockout cells, we evaluated mRNA expression of *NTRK1, NTRK2*, and *NTRK3* in MOLM-13 and MV4-11 cells with and without *TP53* deletion. Although *NTRK1* and *NTRK2* were expressed at lower levels in KO cells, *NTRK3* RNA was highly expressed in *TP53* KO cells, indicating a transcriptional component of *NTRK3* upregulation (Fig. 7E). *NTRK1* was expressed at a lower level, albeit higher, in control cells, explaining sensitivity to entrectinib, whereas in *TP53* KO cells the mRNA expression switches to *NTRK3*. Analyses of TRK protein levels revealed increases in overall and phosphorylated levels of TRK proteins in the p53 loss-of-function setting, and we observed significant

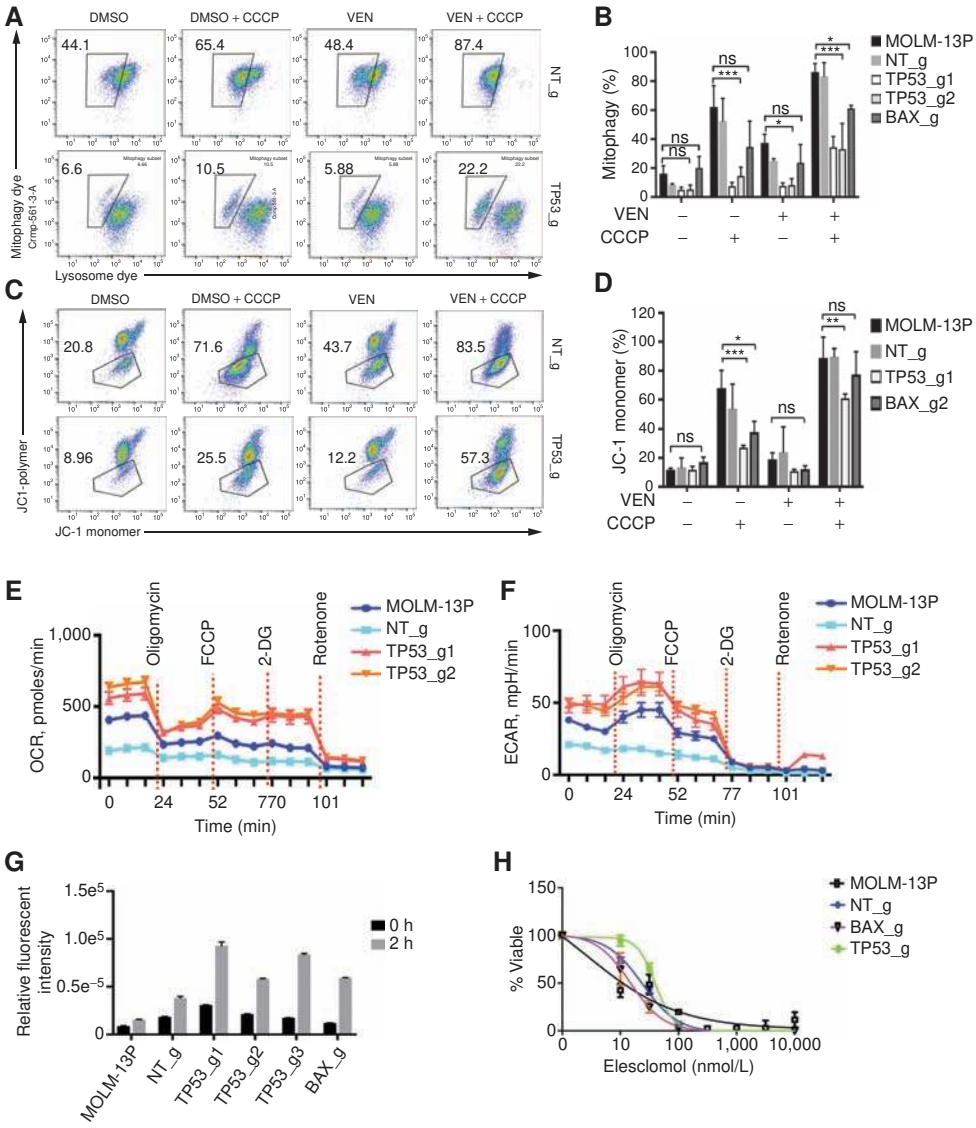

Figure 5. Cells with *TP53* and *BAX* inactivation are resistant to mitochondrial stress induced by venetoclax and mitochondrial uncouplers. **A,** Flow cytometry analyses of MOLM-13 nontargeting and MOLM-13 *TP53* KO cells for mitophagy with and without initial 2-hour stimulation with 100 nmol/L venetoclax and/or CCCP. Ten thousand cells were analyzed. Box drawn around doubly stained brighter cells with mitophagy dye is a result of acidification of the mitophagy dye in lysosomes after fusion with damaged mitochondria. **B,** Histogram of mitophagy experiments ($n = 3$). Statistical significance determined by ANOVA with Tukey post-test. Note that the number of mitochondria fused to lysosomes is significantly less in MOLM-13 cells with *TP53* knockout (TP53_g) and *BAX* (BAX_g) relative to control parental and nontargeting (NT_g) cells in the presence of uncoupler CCCP with and without venetoclax (VEN). *, $P < 0.05$; **, $P = 0.01$; ***, $P < 0.001$; ns, not significant. **C**. Flow cytometry analyses of mitochondrial depolarization. Percentage of cells with depolarized mitochondria in response to mitochondrial uncoupler CCCP is shown (boxed region: green fluorescent cells representing monomer form of cationic carbocyanine dye JC-1 in depolarized cells). Red fluorescent cells represent polymeric form of JC-1 in hyperpolarized cells. Note protection against depolarization in *TP53* and *BAX* KO cells. **D,** Histogram of experiments shown in **C** ($n = 3$) with 10,000 cells analyzed per sample. Statistical significance determined by ANOVA with Tukey post-test. *, $P < 0.05$; **, $P = 0.01$; ***, $P < 0.001$; ns, not significant. **E, F,** Analyses of oxygen consumption rate (OCR) and extracellular acidification rates (ECAR) using Seahorse assay ($n = 3$). **G,** Measurement of ROS using 2′,7′-dichlorofluorescin diacetate (DCFDA, Abcam) substrate as an indicator of oxidation inside the cell detected by conversion to fluorescent DCF compound. Note higher rate of ROS in *TP53* and *BAX* KO cells ($n = 6$). **H,** Cell viability assay in response to elesclomol.

decreases in phosphorylation of TRK and downstream MAPK signaling in response to treatment with entrectinib in *TP53* KO MOLM-13 cells, but not in control or parental cells (Fig. 7F). Treatment of *TP53* KO cells with entrectinib resulted in G_1 cell-cycle blockade (Supplementary Fig. S5A and S5B), and treatment of these cells with entrectinib and venetoclax together was effective in both parental and *TP53* KO cell lines but not synergistic relative to each single agent (Supplementary Fig. S5C). Analysis of cell lysates obtained from AML patient samples revealed a marked increase in TRK protein with detectable levels of phosphorylated pan-TRK and TRKC in *TP53*-mutant versus undetectable levels in WT cases (Fig. 7G). *Ex vivo* analysis of leukemic blasts from these patients with AML showed increased sensitivity to entrectinib in those samples harboring *TP53* mutations (Supplementary Fig. S6A). A preliminary patient-derived xenograft

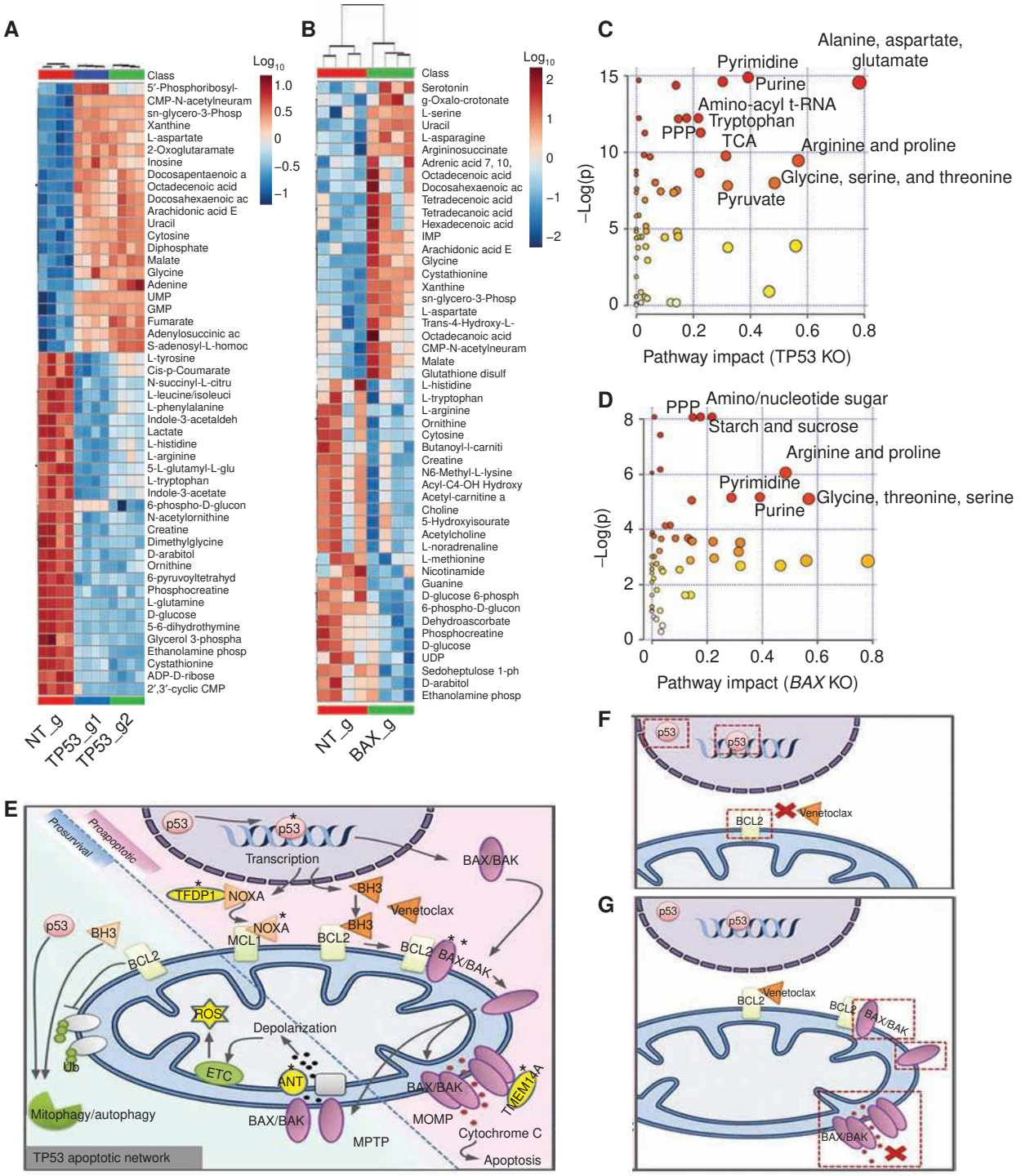

Figure 6. Metabolic changes in *TP53* and *BAX* KO cells are indicative of increased cell proliferation. **A** and **B**, Global metabolomics profile of MOLM-13 *TP53* (**A**) and *BAX* KO (**B**) cells. Metabolomic analysis was performed on samples in quadruplicate. Top 50 changed metabolites are shown. **C** and **D**, Pathway analysis of metabolites with differential abundance dot plot for MOLM-13 *TP53* (**C**) and *BAX* KO (**D**) cells. Red to yellow color gradient indicates higher to lower statistical significance; circle size is proportional to the percentage of affected metabolites within the pathway. **E,** Summary of genes identified by the CRISPR/Cas9 screen affecting mitochondrial homeostasis, energy production, apoptosis, and venetoclax response. Star symbol indicates identified genes: *TP53* (p53), *TFDP1* (DP-1), *NOXA* (PMAIP1), *BAX/BAK*, *TMEM14A*, *SLC25A6* (ANT3). Mechanisms of venetoclax resistance in cells with inactivation of *TP53* (**F**) or *BAX* (**G**). Inactivation of *TP53* leads to perturbation in the expression of prosurvival proteins, including BCL2, the primary venetoclax target. Inactivation of *BAX* leads to inability to build effective mitochondrial outer membrane permeabilization (MOMP) during apoptosis, induced by venetoclax.

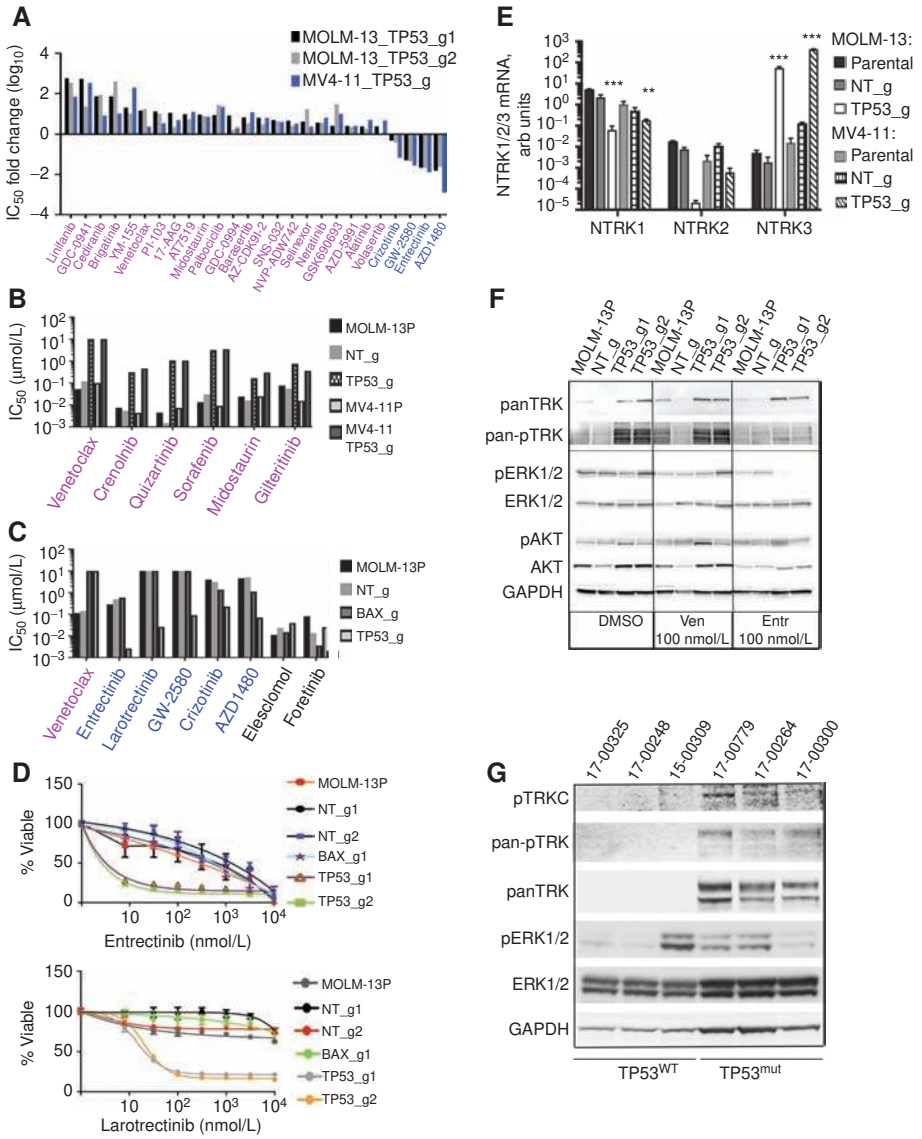

Figure 7. Cells with loss-of-function alleles for *TP53* or *BAX* have altered sensitivities to small-molecule inhibitors of various signaling pathways. **A,** MOLM-13 and MV4-11 cells, transduced with indicated sgRNAs/Cas9 viruses, were screened with a panel of inhibitors targeting various molecular pathways and assessed using the drug-screening method described in Fig. 2A. Fold changes in IC_{50} values (log_{10} scale) for those inhibitors concordant across both cell lines relative to nontargeting controls are shown. **B,** Analyses of FLT3 inhibitor sensitivities, in MOLM-13 and MV4-11 parental and KO cells, as indicated. Drug sensitivity was measured as described in Fig. 2A, with IC_{50} estimated from triplicates. **C,** Histogram of sensitivities (IC_{50} values) to a series of NTRK inhibitors in MOLM-13 cells, transduced with indicated sgRNAs/Cas9 viruses. **D,** Drug sensitivity to NTRK inhibitors entrectinib (top) and larotrectinib (bottom) as measured in Fig. 2A and F, in MOLM-13 cells transduced with indicated sgRNAs/Cas9 viruses. **E,** Expression levels of NTRK1, 2 and 3 mRNA using qRT-PCR analysis with RNAs isolated from MOLM-13 and MV4-11 cells with *TP53* KO alleles or nontargeting (NT) control. Expression values were normalized to 36B4 gene-expression levels. Statistical significance was determined by ANOVA with Tukey post-test (**, $P < 0.01$; ***, $P < 0.001$). **F,** Western blot analyses of proteins extracted from MOLM-13 parental and MOLM-13 transduced with *TP53* sgRNA/Cas9 viruses and treated overnight with venetoclax (Ven; 100 nmol/L), entrectinib (Entr; 100 nmol/L), or vehicle (DMSO) and identified with antisera to pan-NTRK, phosphorylated NTRK (Tyr516), phosphorylated ERK1/2 (Thr202/Tyr204), ERK1/2, phosphorylated AKT (Thr308), AKT, and GAPDH. **G,** Western blot analyses of proteins from AML patient samples with known *TP53*-mutant ($TP53^{mut}$) or WT ($TP53^{WT}$) status. Samples 17-00248 and 15-00309 have FLT3-ITD mutations; sample 17-00300 has a $FLT3^{D835E}$ mutation.

study using two independent *TP53*-mutant samples showed a response to entrectinib treatment as detected by reduced spleen weight and disease burden relative to vehicle control (Supplementary Fig. S6B).

Together, these data have identified a mechanism of venetoclax resistance in AML, namely, the p53 apoptosis machinery, and demonstrated an approach to identify and validate candidate genes involved in drug resistance. In addition, our data suggest a dependency on new survival pathways (e.g., NTRK) in *TP53*-mutant cells and patients. Cells resistant to venetoclax exhibited perturbations in mitochondrial homeostasis, were abnormally protective in responses to various mitochondrial stressors, and exhibited significant metabolic differences, indicative of high proliferation rates, energy production, and DNA synthesis. These metabolic differences were echoed in AML patient samples with *TP53* mutations.

DISCUSSION

Venetoclax therapy for CLL has produced durable responses in a majority of patients (79%), with complete response in 20% of patients (60). Venetoclax has shown limited success in AML clinical trials as a single agent due to drug resistance in the majority of patients (24). Both of these clinical results are mirrored in venetoclax sensitivity observed *ex vivo* in patient samples assayed in the Beat AML cohort (40), where we observed greater activity of venetoclax on CLL (141 patients) than on AML (289 patients) specimens, with a median IC_{50} for AML significantly higher than that for CLL (1.4 μmol/L vs. 0.1 μmol/L, respectively; Mann–Whitney $P < 0.001$). The efficacy of venetoclax in newly diagnosed patients with AML, when administered in combination with azacytidine, has been more robust, although the *TP53*-mutant subset exhibited the worst response rate of any subset of patients reported in the study (25, 61), and this combination, as well as other venetoclax combinations, is likely to see broader use in AML and in CLL, prompting a need to better understand possible mechanisms of resistance. Our findings identify genes affecting control and execution of apoptosis in mitochondria (*TP53, BAX*, and *PMAIP1*); their inactivation individually establishes venetoclax resistance in AML cell lines. These results correlate with a recent study reporting activation of p53 through inhibition of MDM2 overcomes venetoclax resistance in AML cell lines (30). The mechanism of venetoclax action is concentrated on the mitochondria, a center of energy production through cellular respiration as well as initiation of apoptosis; its target, BCL2, functions in both cell survival and the oxidative phosphorylation process. In many ways, homeostasis of mitochondria and cell survival in apoptosis are tightly linked. Attesting to this point, venetoclax-resistant cells show both: likely resistance through changes in expression of prosurvival and proapoptotic proteins and perturbation in mitochondrial stress sensitivities.

Loss of p53 Affects Sensitivity to Other Signaling Pathway Inhibitors

Loss of p53 affected drug sensitivities to a wide range of small molecules, including FLT3 inhibitors. Many tyrosine kinase inhibitors have multiple targets, making it difficult to dissect sensitivity change unless a group of related inhibitors is affected. For example, a previous study of patients with relapsed/refractory AML with newly acquired crenolanib resistance identified *TP53* mutations associated with resistance (62). Our results expand on that finding and include loss of sensitivity changes for many FLT3 inhibitors, an observation that is likely due to disruption of the normal apoptotic response in *TP53*-mutant cells. Additionally, we observed a new dependency on the NTRK pathway, which was confirmed by a similar increase in sensitivity to several inhibitors, either affecting NTRK/ALK/ROS1 signaling such as entrectinib, or the NTRK-selective inhibitor larotrectinib. *TP53* mutations in AML are typically rare (<8% of all cases); however, a dysfunctional WT *TP53* is much more common and requires functional assessment of *TP53*. In general, *TP53* mutations confer poor prognosis and reduced sensitivity to a variety of small molecules, and frequently associate with relapsed/refractory AML cases (62).

Our future studies will focus on assessing NTRK inhibitor sensitivity in *TP53*-mutant AML patient sample xenografts. The detection of the TRK receptors on immature leukemic cell lines demonstrated that NTRK1 expression and activation are not restricted to the nervous system, but are also an important element in early hematopoiesis (63). TRK receptors, which promote the proliferation and survival of erythroblasts, dendritic cells, lymphocytes, monocytes, and macrophages (64), have also been detected in human bone marrow cells (65). TRK expression occurs in myeloid leukemia cell lines and in primary leukemic cells from patients with AML (66). Subsequent studies have shown that activation of TRK receptors in hematologic malignancies could result from chromosomal rearrangements (67), point mutations (68), truncations (69), and transcriptional changes (70). Although the prevalence of NTRK-mediated cancers is <1%, fusions involving NTRK3 were observed in various hematologic malignancies including AML (67). The efficacy of TRK inhibitors has been demonstrated in NTRK fusion–positive human leukemia cell lines and patient-derived xenograft studies, highlighting the potential clinical utility of these inhibitors for a subset of patients with leukemia (71, 72).

In our study, sensitivity to TRK inhibitors correlated with an increase in expression of NTRK3 and a concomitant decrease in NTRK1 in *TP53* KO cells at the RNA and protein levels, indicating a transcriptional regulation. We also observed increased TRK protein levels in *TP53*-mutant patient samples. Among genes that regulate NTRK expression, RUNX family proteins bind *NTRK* loci (73) and have regulatory roles in both hematopoietic development and cancer (74). *RUNX1* (AML1), a frequently mutated gene in AML, is often disrupted by translocation (75). *RUNX1* isoforms can either enhance or repress gene expression in AML cell lines (76) with isoform *RUNX1A* having a repressor function due to the absence of its C-terminal transactivation domain. AML1 expression is decreased in both *TP53*-mutant patient samples and *TP53* KO cell lines (Supplementary Fig. S6C and S6D), suggesting a potential mechanism whereby the interplay between various RUNX isoforms may regulate NTRK expression levels. In mice, p53 binds to the distal *Runx1* promoter, leading to AML1 upregulation and lymphoma development (77). Future studies will examine whether *NTRK* loci occupancy with various *RUNX1* isoforms leads to upregulation of specific NTRKs in *TP53*-mutant cells.

Genome-Wide Screen Identified Genes Controlling Proapoptotic Responses and Mitochondria Functions

Our screen identified genes whose inactivation confers venetoclax resistance. The most significant hits have a similar mode of action in apoptosis, namely, a strong proapoptotic activity. These included p53, a transcription factor with both activating and repressing functions controlling many aspects of cellular responses, including genotoxic stress pertinent to apoptotic signaling, and several p53 transcriptional targets, *BAX*, *BAK1*/*BAK*, and *PMAIP1* (37, 78, 79). We found changes in the gene expression of several p53-regulated genes altered in our *TP53* KO MOLM-13 cells, including proapoptotic *PMAIP1*, *BAK1*, and *PUMA*, without notable changes to BAX expression. BAX and BAK are critical for both mitochondrial outer membrane permeabilization (MOMP) in apoptosis and mitochondrial permeability transition pore (MPTP) formation. PMAIP1 senses apoptotic signaling and inhibits MCL1. TFDP1, together with E2F1, activates and translocates PMAIP1 into mitochondria

(80), and SLC25A6 (ANT3), a nucleotide ADP/ATP translocase that is involved in formation of MPTP, is important for depolarization in mitochondrial recycling (refs. 81–83; Fig. 6E). Importantly, venetoclax induced membrane depolarization in control cells (Fig. 5) and showed synergy with CCCP in mutant cells, suggesting that it is part of its mechanism of action. In fact, we found that mitochondria in venetoclax-resistant cells show a different response to mitochondrial stress, and both *TP53*- and *BAX*-mutant cells had decreased mitophagy and exhibited membrane depolarization protection.

In *TP53* KO cells, we found changes beyond direct p53 target genes. These included downregulation of BCL2 and MCL1 and significant upregulation of BCLXL, without notable changes to BAX expression. With the exception of MCL1, the upregulation of BCLXL and downregulation of BCL2 correlate well with expression levels of p53 in a large AML cohort (40) as well as in pediatric acute lymphoblastic leukemia (39). These alterations in expression of proapoptotic proteins may reflect compensatory changes. *TP53* KO cells were sensitive to the BCL2/BCLXL inhibitor (AZD-4320); however, *BAX* KO cells were 10-fold less sensitive. In contrast, *TP53* KO, but not *BAX* KO, cells were less sensitive to a selective MCL1 inhibitor (AZD-5991). These differences may reflect upregulation of BCLXL and a decrease in MCL1 levels in *TP53* KO cells but not in *BAX* KO cells. With regard to *BAX* KO insensitivity to venetoclax, although both BAX and BAK can result in MOMP, our data may suggest functional differences between BCL2-driven and MCL1-driven BAX and BAK inhibition. The mechanism may involve localization of BAX (cytosolic) and BAK (mitochondrial) prior to the oligomerization processes required for MOMP.

Metabolic Changes in Venetoclax-Resistant Cells Likely Reflect an Increased Proliferation Rate in *TP53* and *BAX* KO Cells with Defective Apoptosis

Metabolic profiling of our mutant cells further indicated changes in energy utilization. Perturbations in the metabolism of cancer cells have been long recognized; for example, some cancer cells rely on glycolysis and pentose phosphate pathways versus cellular respiration, known as the Warburg effect (48). This phenomenon is directed toward utilization of carbon sources for nucleotides, fatty acid and protein synthesis required for cellular proliferation. Although MOLM-13 cells are leukemia-derived with a cancer metabolism, inactivation of p53 and BAX further exacerbated metabolic changes: Increased cellular proliferation led to a diversion of resources into production of nucleotides, fatty acids, and proteins required for membrane production. Curiously, this was accompanied by increased cellular respiration/increase in ROS production relative to parental cells, suggesting that mitochondria are overcompensating for the glycolysis intermediates shunting into the pentose phosphate pathway. Similar metabolic changes, accompanied by increased oxidative phosphorylation as a result of p53 inactivation, were previously observed in other tissues (84). It is possible that p53 inactivation also has a transcriptional impact on the observed metabolic changes, because it is known to negatively control glycolysis through the induction of TIGAR expression (45), which degrades fructose-2,6-bisphosphate and opposes the Warburg effect. Similarly, the *TP53–PUMA* axis has been implicated in metabolic switching toward suppressing oxidative phosphorylation and glycolysis correlating with decreased levels of PUMA in *TP53* KO cells and the observed metabolic changes (44). Several other changes in metabolic profile, namely increases or decreases in several amino acids (variable between *TP53*- and *BAX*-mutant cells) and urea cycle intermediates (common to both *TP53*- and *BAX*-mutant cells), suggest the presence of other catabolic shunts to provide carbon sources for amino acids necessary for new cell production. Metabolic perturbations similar to those observed in *TP53* KO cells were found in our primary AML patient samples. It has been observed that treatment of leukemic stem cells (LSC) from newly diagnosed patients with AML with venetoclax and a DNMT inhibitor (DNMTi) leads to reduced amino acid levels, inhibition of oxidative phosphorylation, and cell death (43). Furthermore, LSCs obtained from patients with AML are resistant to venetoclax and a DNMTi due to their ability to compensate for amino acid loss by increasing fatty-acid metabolism (43), an effect we also observed in *TP53* KO cells and in AML patient samples. Given that DNMTi incorporate into DNA and inhibit DNA methylation, it may be that the increased nucleotide synthesis observed in *TP53* KO cells elevates competition between nucleotides and chemical nucleotide analogues, thereby rendering DNMT inhibitors less effective.

Clinically Relevant Hits Are Identified within the Beat AML Dataset

Identification of a significant collection of apoptosis and mitochondria homeostasis controlling genes in our genome-wide screen for venetoclax resistance validated our top hit findings. However, although they provide mechanistic insight, some validated hits do not correlate with available patient sample data. For example, we did not find a correlation between low PMAIP1 expression and low venetoclax sensitivity in our AML patient cohort, nor were mutations in *PMAIP1* associated with loss of venetoclax sensitivity, underlying the importance of leveraging an independent patient data resource to the screen. Although some hits identified in the screen are not represented as either mutations or low expressers in the Beat AML dataset, collectively they identify the larger network of genes mechanistically responsible for venetoclax sensitivity. Although we focused on the loss of function of genes conferring venetoclax resistance, our screen predicts that gain-of-function mutations in prosurvival genes in the apoptotic cascade will also result in resistance to venetoclax. Notably, a companion study in this issue by Chen and colleagues, where the focus of investigation was on a discovery of venetoclax-sensitizing genes, revealed genes in pertinent mitochondrial functions. Further analysis of the venetoclax-sensitizing genes in this companion study uncovered impacts on mitochondrial function and metabolic pathways that were opposite to the affects observed with venetoclax-resistance genes here. Collectively, these data suggest that mitochondrial function and specific metabolic pathways are essential in governing both sensitization and resistance to venetoclax.

Recent clinical trial success with the combination of venetoclax and a DNMTi (25) identified lower response rates in patients with *TP53* mutations than in the overall cohort (47% vs. ~70% overall), aligning with our findings here. Indeed, patients in the *TP53* mutations subset exhibited the worst response rate of any subset of patients reported in the study with all other molecular/clinical groups in the study exhibiting 60% to 91% complete response/complete response with incomplete blood

count recovery (CR/CRi) rate (including the poor cytogenetic risk group). Further, the *TP53*-mutant patient group had the lowest odds ratio for CR/CRi response and was the only variable that significantly correlated with worse response. A longer study may elucidate whether those *TP53*-mutant patients receiving the combination treatment will relapse at a higher rate, possibly with a clone that has higher allele frequency *TP53* mutation.

METHODS

A complete Methods section is provided in Supplementary Material.

Cell Lines

Human MOLM-13 cells were obtained from the Sanger Institute Cancer Cell Line Panel. Human MV4-11, OCI-AML2, and THP-1 were obtained from ATCC. Authentication was performed on all cell lines used in this study at the Oregon Health and Science University (OHSU) DNA Services Core facility. All cell lines were tested for *Mycoplasma* on a monthly schedule.

CRISPR/Cas9 Screen

Loss-of-function screens were performed using two human genome-wide sgRNA libraries—Y. Kosuke library (31) and Brunello library (33)—both purchased form Addgene (#73179 and #67989, respectively).

Biostatistical Analysis

Pipeline for executing analyses of CRISPR library sequences was performed using MAGeCK analyses (32).

Ex Vivo *Functional Screen*

Small-molecule inhibitors, purchased from LC Laboratories Inc. and Selleck Chemicals, were reconstituted in DMSO and stored at −80°C.

Xenograft Generation

Animal studies were conducted with approval from the OHSU Institutional Animal Care and Use Committee. Patient samples were injected into cohorts of NSGS mice and allowed to engraft until the peripheral blood showed approximately 1% human CD33 chimerisms.

Metabolomic Analysis

Two million MOLM-13 and MV4-11 cells were flash-frozen as cell pellet and metabolomics analyses were performed via ultra-high-pressure liquid chromatography–mass spectrometry (UHPLC-MS; Vanquish and Q Exactive, Thermo Fisher) as previously reported (85).

Mitophagy Detection

Cells were loaded in complete medium with 100 nmol/L Mitophagy Dye (Mitophagy Detection Kit, Dojindo Molecular Technologies). The data were analyzed post acquisition using FlowJo software (Tree Star). Ten thousand cells were acquired using channels 405-2-A (lyso Dye), 561-3-A (Mitophagy Dye), and 640-1-A (MitoTracker Dye).

Mitochondrial Membrane Potential

Mitochondrial membrane potential was assessed using tetramethylrhodamine methyl ester bound to cationic carbocyanine (JC-1, Dojingo Molecular Technology). Cells were treated with 100 nmol/L venetoclax or DMSO and with or without CCCP for 2 hours prior to the addition of the dye and flow cytometry.

Data Availability

Raw data files for CRISPR screens have been deposited at the Gene Expression Omnibus and can be found under the accession number GSE130414.

Disclosure of Potential Conflicts of Interest

A.V. Danilov has received commercial research grants from Gilead Sciences, Verastem, Takeda, AstraZeneca, and Verastem Oncology, and is a consultant/advisory board member for AbbVie, AstraZeneca, Genentech, Verastem Oncology, Seattle Genetics, TG Therapeutics, Curis, Celgene, Teva Oncology, and Gilead Sciences. B.J. Druker serves on the board of directors of Amgen, Burroughs Wellcome Fund, and CureOne; reports receiving other commercial research support from Novartis, Bristol-Myers Squibb, and Pfizer (institutional funding—PI or co-investigator on clinical trials funded via contract with OHSU); has ownership interest (including stock, patents, etc.) in Amgen, Blueprint Medicines, MolecularMD (inactive—acquired by ICON Laboratories), GRAIL, Patent 6958335 (exclusively licensed to Novartis), Henry Stewart Talks, Merck via Dana-Farber Cancer Institute (royalty payments); is a consultant/advisory board member for Aileron Therapeutics, ALLCRON, Third Coast Therapeutics, Vivid Biosciences, Monojul (inactive), Baxalta (inactive), CTI Biopharma (inactive), Aptose, Beta Cat, Blueprint Medicines, Celgene, Cepheid, GRAIL (former), Gilead (former), and Patient True Talk; and is an uncompensated joint steering committee member for Beat AML LLC. J.W. Tyner has received commercial research grants from Agios, Aptose, Array, AstraZeneca, Constellation, Genentech, Gilead, Incyte, Janssen, Seattle Genetics, Syros, and Takeda; has received honoraria from the speakers bureaus of Therapeutic Advances in Childhood Leukemia and Hermedicus - Acute Leukemia Forum; has ownership interest in Vivid Biosciences; and is a consultant/advisory board member of Vivid Biosciences. No potential conflicts of interest were disclosed by the other authors.

Authors' Contributions

Conception and design: T. Nechiporuk, S.E. Kurtz, C.E. Tognon, J.W. Tyner
Development of methodology: T. Nechiporuk, T. Liu, A. D'Alessandro, S.K. Joshi
Acquisition of data (provided animals, acquired and managed patients, provided facilities, etc.): T. Nechiporuk, S.E. Kurtz, T. Liu, C.L. Jones, A. D'Alessandro, A. d'Almeida, S.K. Joshi, A.V. Danilov, B.H. Chang
Analysis and interpretation of data (e.g., statistical analysis, biostatistics, computational analysis): T. Nechiporuk, S.E. Kurtz, O. Nikolova, T. Liu, A. D'Alessandro, R. Culp-Hill, S.K. Joshi, M. Rosenberg, A.V. Danilov, J.W. Tyner
Writing, review, and/or revision of the manuscript: T. Nechiporuk, S.E. Kurtz, O. Nikolova, T. Liu, R. Culp-Hill, S.K. Joshi, C.E. Tognon, B.J. Druker, B.H. Chang, J.W. Tyner
Administrative, technical, or material support (i.e., reporting or organizing data, constructing databases): T. Nechiporuk, R. Culp-Hill, J.W. Tyner
Study supervision: A. D'Alessandro, B.J. Druker, J.W. Tyner
Other (development of prioritization framework to assist in rigor and reproducibility): S.K. McWeeney

Acknowledgments

We thank Wesley Horton and Kevin Watanabe-Smith for analytical support and the OHSU Massively Parallel Sequencing Shared Resource and Flow Cytometry Core for technical support. This study was also supported by grants from the NCI (1U01CA217862, 1U54CA224019, and 3P30CA069533-18S5). J.W. Tyner received grants from the V Foundation for Cancer Research, the Gabrielle's Angel Foundation for Cancer Research, and the NCI (1R01CA183947). S.K. Joshi is supported by the ARCS Scholar Foundation and the NCI (1F30CA239335-10).

The costs of publication of this article were defrayed in part by the payment of page charges. This article must therefore be hereby marked *advertisement* in accordance with 18 U.S.C. Section 1734 solely to indicate this fact.

Received January 30, 2019; revised April 20, 2019; accepted April 30, 2019; published first May 2, 2019.

REFERENCES

1. Hanahan D, Weinberg RA. Hallmarks of cancer: the next generation. Cell 2011;144:646–74.
2. Llambi F, Green DR. Apoptosis and oncogenesis: give and take in the BCL-2 family. Curr Opin Genet Dev 2011;21:12–20.
3. Hata AN, Engelman JA, Faber AC. The BCL2 family: key mediators of the apoptotic response to targeted anticancer therapeutics. Cancer Discov 2015;5:475–87.
4. Letai AG. Diagnosing and exploiting cancer's addiction to blocks in apoptosis. Nat Rev Cancer 2008;8:121–32.
5. Khoo KH, Verma CS, Lane DP. Drugging the p53 pathway: understanding the route to clinical efficacy. Nat Rev Drug Discov 2014; 13:217–36.
6. Haupt Y, Maya R, Kazaz A, Oren M. Mdm2 promotes the rapid degradation of p53. Nature 1997;387:296–9.
7. Wertz IE, Kusam S, Lam C, Okamoto T, Sandoval W, Anderson DJ, et al. Sensitivity to antitubulin chemotherapeutics is regulated by MCL1 and FBW7. Nature 2011;471:110–4.
8. Rochaix P, Krajewski S, Reed JC, Bonnet F, Voigt JJ, Brousset P. In vivo patterns of Bcl-2 family protein expression in breast carcinomas in relation to apoptosis. J Pathol 1999;187:410–5.
9. Zhang B, Gojo I, Fenton RG. Myeloid cell factor-1 is a critical survival factor for multiple myeloma. Blood 2002;99:1885–93.
10. Beroukhim R, Mermel CH, Porter D, Wei G, Raychaudhuri S, Donovan J, et al. The landscape of somatic copy-number alteration across human cancers. Nature 2010;463:899–905.
11. Kojima K, Konopleva M, McQueen T, O'Brien S, Plunkett W, Andreeff M. Mdm2 inhibitor Nutlin-3a induces p53-mediated apoptosis by transcription-dependent and transcription-independent mechanisms and may overcome Atm-mediated resistance to fludarabine in chronic lymphocytic leukemia. Blood 2006;108:993–1000.
12. Hasegawa H, Yamada Y, Iha H, Tsukasaki K, Nagai K, Atogami S, et al. Activation of p53 by Nutlin-3a, an antagonist of MDM2, induces apoptosis and cellular senescence in adult T-cell leukemia cells. Leukemia 2009;23:2090–101.
13. Tait SW, Green DR. Mitochondria and cell death: outer membrane permeabilization and beyond. Nat Rev Mol Cell Biol 2010;11:621–32.
14. Juin P, Geneste O, Gautier F, Depil S, Campone M. Decoding and unlocking the BCL-2 dependency of cancer cells. Nat Rev Cancer 2013;13:455–65.
15. Oltersdorf T, Elmore SW, Shoemaker AR, Armstrong RC, Augeri DJ, Belli BA, et al. An inhibitor of Bcl-2 family proteins induces regression of solid tumours. Nature 2005;435:677–81.
16. Souers AJ, Leverson JD, Boghaert ER, Ackler SL, Catron ND, Chen J, et al. ABT-199, a potent and selective BCL-2 inhibitor, achieves antitumor activity while sparing platelets. Nat Med 2013;19:202–8.
17. Caenepeel S, Brown SP, Belmontes B, Moody G, Keegan KS, Chui D, et al. AMG 176, a Selective MCL1 inhibitor, is effective in hematologic cancer models alone and in combination with established therapies. Cancer Discov 2018;8:1582–1597.
18. Kotschy A, Szlavik Z, Murray J, Davidson J, Maragno AL, Le Toumelin-Braizat G, et al. The MCL1 inhibitor S63845 is tolerable and effective in diverse cancer models. Nature 2016;538:477–482.
19. Ramsey HE, Fischer MA, Lee T, Gorska AE, Arrate MP, Fuller L, et al. A Novel MCL1 inhibitor combined with venetoclax rescues venetoclax-resistant acute myelogenous leukemia. Cancer Discov 2018;8: 1566–1581.
20. Tron AE, Belmonte MA, Adam A, Aquila BM, Boise LH, Chiarparin E, et al. Discovery of Mcl-1-specific inhibitor AZD5991 and preclinical activity in multiple myeloma and acute myeloid leukemia. Nat Commun 2018;9:5341.
21. Pan R, Hogdal LJ, Benito JM, Bucci D, Han L, Borthakur G, et al. Selective BCL-2 inhibition by ABT-199 causes on-target cell death in acute myeloid leukemia. Cancer Discov 2014;4:362–75.
22. Roberts AW, Davids MS, Pagel JM, Kahl BS, Puvvada SD, Gerecitano JF, et al. Targeting BCL2 with venetoclax in relapsed chronic lymphocytic leukemia. N Engl J Med 2016;374:311–22.
23. Seymour JF, Ma S, Brander DM, Choi MY, Barrientos J, Davids MS, et al. Venetoclax plus rituximab in relapsed or refractory chronic lymphocytic leukaemia: a phase 1b study. Lancet Oncol 2017;18:230–240.
24. Konopleva M, Pollyea DA, Potluri J, Chyla B, Hogdal L, Busman T, et al. Efficacy and biological correlates of response in a phase II study of venetoclax monotherapy in patients with acute myelogenous leukemia. Cancer Discov 2016;6:1106–1117.
25. DiNardo CD, Pratz KW, Letai A, Jonas BA, Wei AH, Thirman M, et al. Safety and preliminary efficacy of venetoclax with decitabine or azacitidine in elderly patients with previously untreated acute myeloid leukaemia: a non-randomised, open-label, phase 1b study. Lancet Oncol 2018;19:216–228.
26. Holohan C, Van Schaeybroeck S, Longley DB, Johnston PG. Cancer drug resistance: an evolving paradigm. Nat Rev Cancer 2013;13:714–26.
27. Phillips DC, Xiao Y, Lam LT, Litvinovich E, Roberts-Rapp L, Souers AJ, et al. Loss in MCL-1 function sensitizes non-Hodgkin's lymphoma cell lines to the BCL-2-selective inhibitor venetoclax (ABT-199). Blood Cancer J 2015;5:e368.
28. Bodo J, Zhao X, Durkin L, Souers AJ, Phillips DC, Smith MR, et al. Acquired resistance to venetoclax (ABT-199) in t(14;18) positive lymphoma cells. Oncotarget 2016;7:70000–70010.
29. Lin KH, Winter PS, Xie A, Roth C, Martz CA, Stein EM, et al. Targeting MCL-1/BCL-XL forestalls the acquisition of resistance to ABT-199 in acute myeloid leukemia. Sci Rep 2016;6:27696.
30. Pan R, Ruvolo V, Mu H, Leverson JD, Nichols G, Reed JC, et al. Synthetic lethality of combined Bcl-2 inhibition and p53 activation in AML: mechanisms and superior antileukemic efficacy. Cancer Cell 2017;32:748–760.
31. Tzelepis K, Koike-Yusa H, De Braekeleer E, Li Y, Metzakopian E, Dovey OM, et al. A CRISPR dropout screen identifies genetic vulnerabilities and therapeutic targets in acute myeloid leukemia. Cell Rep 2016;17:1193–1205.
32. Li W, Xu H, Xiao T, Cong L, Love MI, Zhang F, et al. MAGeCK enables robust identification of essential genes from genome-scale CRISPR/Cas9 knockout screens. Genome Biol 2014;15:554.
33. Doench JG, Fusi N, Sullender M, Hegde M, Vaimberg EW, Donovan KF, et al. Optimized sgRNA design to maximize activity and minimize off-target effects of CRISPR-Cas9. Nat Biotechnol 2016;34: 184–191.
34. Woo IS, Jin H, Kang ES, Kim HJ, Lee JH, Chang KC, et al. TMEM14A inhibits N-(4-hydroxyphenyl)retinamide-induced apoptosis through the stabilization of mitochondrial membrane potential. Cancer Lett 2011;309:190–8.
35. Hershko T, Ginsberg D. Up-regulation of Bcl-2 homology 3 (BH3)-only proteins by E2F1 mediates apoptosis. J Biol Chem 2004;279:8627–34.
36. Imazu T, Shimizu S, Tagami S, Matsushima M, Nakamura Y, Miki T, et al. Bcl-2/E1B 19 kDa-interacting protein 3-like protein (Bnip3L) interacts with bcl-2/Bcl-xL and induces apoptosis by altering mitochondrial membrane permeability. Oncogene 1999;18:4523–9.
37. Fischer MCensus and evaluation of p53 target genes. Oncogene 2017; 36:3943–3956.
38. Kojima K, Konopleva M, Samudio IJ, Shikami M, Cabreira-Hansen M, McQueen T, et al. MDM2 antagonists induce p53-dependent apoptosis in AML: implications for leukemia therapy. Blood 2005;106:3150–9.
39. Findley HW, Gu L, Yeager AM, Zhou M. Expression and regulation of Bcl-2, Bcl-xl, and Bax correlate with p53 status and sensitivity to apoptosis in childhood acute lymphoblastic leukemia. Blood 1997;89: 2986–93.
40. Tyner JW, Tognon CE, Bottomly D, Wilmot B, Kurtz SE, Savage SL, et al. Functional genomic landscape of acute myeloid leukaemia. Nature 2018;562:526–531.
41. Blankenberg FG. In vivo detection of apoptosis. J Nucl Med 2008; 49:81s–95s.
42. Lagadinou ED, Sach A, Callahan K, Rossi RM, Neering SJ, Minhajuddin M, et al. BCL-2 inhibition targets oxidative phosphorylation and

selectively eradicates quiescent human leukemia stem cells. Cell Stem Cell 2013;12:329–41.
43. Jones CL, Stevens BM, D'Alessandro A, Reisz JA, Culp-Hill R, Nemkov T, et al. Inhibition of amino acid metabolism selectively targets human leukemia stem cells. Cancer Cell 2018;34:724–740.
44. Kim J, Yu L, Chen W, Xu Y, Wu M, Todorova D, et al. Wild-type p53 promotes cancer metabolic switch by inducing PUMA-dependent suppression of oxidative phosphorylation. Cancer Cell 2019;35:191–203.
45. Bensaad K, Tsuruta A, Selak MA, Vidal MN, Nakano K, Bartrons R, et al. TIGAR, a p53-inducible regulator of glycolysis and apoptosis. Cell 2006;126:107–20.
46. Polyak K, Xia Y, Zweier JL, Kinzler KW, Vogelstein B. A model for p53-induced apoptosis. Nature 1997;389:300–5.
47. Li PF, Dietz R, von Harsdorf R. p53 regulates mitochondrial membrane potential through reactive oxygen species and induces cytochrome c-independent apoptosis blocked by Bcl-2. Embo J 1999;18:6027–36.
48. Vander Heiden MG, Cantley LC, Thompson CB. Understanding the Warburg effect: the metabolic requirements of cell proliferation. Science 2009;324:1029–33.
49. Kirshner JR, He S, Balasubramanyam V, Kepros J, Yang CY, Zhang M, et al. Elesclomol induces cancer cell apoptosis through oxidative stress. Mol Cancer Ther 2008;7:2319–27.
50. Ardini E, Menichincheri M, Banfi P, Bosotti R, De Ponti C, Pulci R, et al. Entrectinib, a pan-TRK, ROS1, ALK inhibitor with activity in multiple molecularly defined cancer indications. Mol Cancer Ther 2016;15:628–39.
51. Vaishnavi A, Capelletti M, Le AT, Kako S, Butaney M, Ercan D, et al. Oncogenic and drug-sensitive NTRK1 rearrangements in lung cancer. Nat Med 2013;19:1469–1472.
52. Taipale M, Krykbaeva I, Whitesell L, Santagata S, Zhang J, Liu Q, et al. Chaperones as thermodynamic sensors of drug-target interactions reveal kinase inhibitor specificities in living cells. Nat Biotechnol 2013;31:630–7.
53. Karaman MW, Herrgard S, Treiber DK, Gallant P, Atteridge CE, Campbell BT, et al. A quantitative analysis of kinase inhibitor selectivity. Nat Biotechnol 2008;26:127–32.
54. Hedvat M, Huszar D, Herrmann A, Gozgit JM, Schroeder A, Sheehy A, et al. The JAK2 inhibitor AZD1480 potently blocks Stat3 signaling and oncogenesis in solid tumors. Cancer Cell 2009;16:487–97.
55. Tognon C, Garnett M, Kenward E, Kay R, Morrison K, Sorensen PH. The chimeric protein tyrosine kinase ETV6-NTRK3 requires both Ras-Erk1/2 and PI3-kinase-Akt signaling for fibroblast transformation. Cancer Res 2001;61:8909–16.
56. Lannon CL, Martin MJ, Tognon CE, Jin W, Kim SJ, Sorensen PH. A highly conserved NTRK3 C-terminal sequence in the ETV6-NTRK3 oncoprotein binds the phosphotyrosine binding domain of insulin receptor substrate-1: an essential interaction for transformation. J Biol Chem 2004;279:6225–34.
57. Davare MA, Tognon CE. Detecting and targeting oncogenic fusion proteins in the genomic era. Biol Cell 2015;107:111–29.
58. Vaishnavi A, Le AT, Doebele RC. TRKing down an old oncogene in a new era of targeted therapy. Cancer Discov 2015;5:25–34.
59. Nakagawara A, Arima-Nakagawara M, Scavarda NJ, Azar CG, Cantor AB, Brodeur GM. Association between high levels of expression of the TRK gene and favorable outcome in human neuroblastoma. N Engl J Med 1993;328:847–54.
60. Edelmann J, Gribben JG. Managing patients with TP53-deficient chronic lymphocytic leukemia. J Oncol Pract 2017;13:371–377.
61. DiNardo CD, Pratz K, Pullarkat V, Jonas BA, Arellano M, Becker PS, et al. Venetoclax combined with decitabine or azacitidine in treatment-naive, elderly patients with acute myeloid leukemia. Blood 2019;133:7–17.
62. Zhang H, Savage S, Schultz AR, Bottomly D, White L, Segerdell E, et al. Clinical resistance to crenolanib in acute myeloid leukemia due to diverse molecular mechanisms. Nat Commun 2019;10:244.
63. Chevalier S, Praloran V, Smith C, MacGrogan D, Ip NY, Yancopoulos GD, et al. Expression and functionality of the trkA proto-oncogene product/NGF receptor in undifferentiated hematopoietic cells. Blood 1994;83:1479–85.
64. Vega JA, García-Suárez O, Hannestad J, Pérez-Pérez M, Germanà A. Neurotrophins and the immune system. J Anat 2003;203:1–19.
65. Labouyrie E, Dubus P, Groppi A, Mahon FX, Ferrer J, Parrens M, et al. Expression of neurotrophins and their receptors in human bone marrow. Am J Pathol 1999;154:405–15.
66. Kaebisch A, Brokt S, Seay U, Lohmeyer J, Jaeger U, Pralle H. Expression of the nerve growth factor receptor c-TRK in human myeloid leukaemia cells. Br J Haematol 1996;95:102–9.
67. Eguchi M, Eguchi-Ishimae M, Tojo A, Morishita K, Suzuki K, Sato Y, et al. Fusion of ETV6 to neurotrophin-3 receptor TRKC in acute myeloid leukemia with t(12;15)(p13;q25). Blood 1999;93:1355–63.
68. Tomasson MH, Xiang Z, Walgren R, Zhao Y, Kasai Y, Miner T, et al. Somatic mutations and germline sequence variants in the expressed tyrosine kinase genes of patients with de novo acute myeloid leukemia. Blood 2008;111:4797–808.
69. Reuther GW, Lambert QT, Caligiuri MA, Der CJ. Identification and characterization of an activating TrkA deletion mutation in acute myeloid leukemia. Mol Cell Biol 2000;20:8655–66.
70. Li Z, Beutel G, Rhein M, Meyer J, Koenecke C, Neumann T, et al. High-affinity neurotrophin receptors and ligands promote leukemogenesis. Blood 2009;113:2028–37.
71. Smith KM, Fagan PC, Pomari E, Germano G, Frasson C, Walsh C, et al. Antitumor activity of entrectinib, a pan-TRK, ROS1, ALK inhibitor, in ETV6-NTRK3-positive acute myeloid leukemia. Mol Cancer Ther 2018;17:455–463.
72. Taylor J, Pavlick D, Yoshimi A, Marcelus C, Chung SS, Hechtman JF, et al. Oncogenic TRK fusions are amenable to inhibition in hematologic malignancies. J Clin Invest 2018;128:3819–3825.
73. Yevshin I, Sharipov R, Kolmykov S, Kondrakhin Y, Kolpakov F. GTRD: a database on gene transcription regulation-2019 update. Nucleic Acids Res 2019;47:D100–d105.
74. Wang Q, Stacy T, Binder M, Marin-Padilla M, Sharpe AH, Speck NA. Disruption of the Cbfa2 gene causes necrosis and hemorrhaging in the central nervous system and blocks definitive hematopoiesis. Proc Natl Acad Sci U S A 1996;93:3444–9.
75. TCGA, genomic and epigenomic landscapes of adult de novo acute myeloid leukemia. N Engl J Med 2013;368:2059–74.
76. Gattenloehner S, Chuvpilo S, Langebrake C, Reinhardt D, Müller-Hermelink HK, Serfling E, et al. Novel RUNX1 isoforms determine the fate of acute myeloid leukemia cells by controlling CD56 expression. Blood 2007;110:2027–33.
77. Shimizu K, Yamagata K, Kurokawa M, Mizutani S, Tsunematsu Y, Kitabayashi I. Roles of AML1/RUNX1 in T-cell malignancy induced by loss of p53. Cancer Sci 2013;104:1033–8.
78. Vogelstein B, Lane D, Levine AJ. Surfing the p53 network. Nature 2000;408:307–10.
79. Levine AJ, Oren M. The first 30 years of p53: growing ever more complex. Nat Rev Cancer 2009;9:749–58.
80. Joshi-Tope G, Gillespie M, Vastrik I, D'Eustachio P, Schmidt E, de Bono B, et al. Reactome: a knowledgebase of biological pathways. Nucleic Acids Res 2005;33(Database issue):D428–32.
81. Palmieri F. The mitochondrial transporter family SLC25: identification, properties and physiopathology. Mol Aspects Med 2013;34:465–84.
82. Verrier F, Mignotte B, Jan G, Brenner C. Study of PTPC composition during apoptosis for identification of viral protein target. Ann N Y Acad Sci 2003;1010:126–42.
83. Rodriguez-Enriquez S, He L, Lemasters JJ. Role of mitochondrial permeability transition pores in mitochondrial autophagy. Int J Biochem Cell Biol 2004;36:2463–72.
84. Prokesch A, Graef FA, Madl T, Kahlhofer J, Heidenreich S, Schumann A, et al. Liver p53 is stabilized upon starvation and required for amino acid catabolism and gluconeogenesis. Faseb j 2017;31:732–742.
85. Nemkov T, D'Alessandro A, Hansen KC. Three-minute method for amino acid analysis by UHPLC and high-resolution quadrupole orbitrap mass spectrometry. Amino Acids 2015;47:2345–57.